J Mater Sci: Mater Electron (2013) 24:5091–5096
DOI 10.1007/s10854-013-1528-0

Effect of film thickness on properties of aluminum doped zinc oxide thin films deposition on polymer substrate

Nihan Akin · S. Sebnem Cetin · Mehmet Cakmak · Tofig Memmedli · Suleyman Ozcelik

Received: 25 July 2013 / Accepted: 3 October 2013 / Published online: 15 October 2013
© Springer Science+Business Media New York 2013

Abstract A series of aluminum doped zinc oxide thin films with different thickness (25–150 nm) were deposited on indium tin oxide coated polyethylene terephthalate substrates by radio frequency magnetron sputtering method at room temperature. The structural, optical and electrical properties of the films were investigated by X-ray Diffractometer, UV–Vis spectrometer and Hall Effect Measurement System. All the obtained films were polycrystalline with a hexagonal structure and a preferred orientation along [002] direction with the c-axis perpendicular to the substrate surface. The optical energy band gap (E_g) values of the films were found to be in the range from 3.36 to 3.26 eV, and their average optical transmissions were about 75 % in the visible region. The films had excellent electrical properties with the resistivities in the range from 2.78×10^{-5} to 2.03×10^{-4} Ω cm, carrier densities more than 3.35×10^{21} cm^{-3} and Hall mobilities between 5.77 and 11.13 cm^2/V s.

1 Introduction

Transparent conducting oxide (TCO) thin films can be successfully used in transparent and flexible optoelectronic device applications such as liquid crystal displays, plasma display panels, electronic paper displays, gas sensor, touch panels, flat panel displays, solar cells and organic light-emitting diodes [1–3]. TCO thin films on polymer substrates have many special merits compared with those on glass, silicon, sapphire and quartz substrates including light weight, small volume, easy portability, flexibility and foldability. These films have a large band gap (>3 eV), low resistivity (>10^{-3} Ω cm) and good optical transmittance (>80 %) in the visible region [4]. The most commonly used TCO thin films are based on tin oxide (TO), indium tin oxide (ITO), cadmium oxide (CdO), zinc oxide (ZnO) or their mixed compounds. In particular, TCO thin films are widely used as transparent conductive electrodes. The characteristics of the films are generally affected by different physical and chemical film deposition techniques based on experimental conditions and requirements such as working pressure, substrate temperature and film thickness [5].

Zinc oxide (ZnO) is a wide band gap (~3.37 eV) semiconductor which has drawn much attention thanks to its large exciton binding energy (~60 meV), high radiation hardness and relatively low growth temperature [6]. Also, it has high optical transparency, non-toxicity, high chemical and mechanical stability, biocompatibility, easy microfabrication processes and abundance availability in the nature [7]. Aluminum (Al), boron (B), indium (In) and gallium (Ga) have been reported as effective dopants for ZnO thin films. Al doped ZnO (AZO) thin films have great effect on optical and electrical properties through band gap modulation, high optical transmittance in UV–VIS–NIR spectrum range and decrease in electrical resistivity. There are many techniques to prepare AZO thin films such as sol–gel processing [8], metal–organic chemical vapor deposition (MOCVD) [9], pulsed laser deposition (PLD) [10], spray pyrolysis [11], direct current (DC) and radio frequency (RF) magnetron sputtering [4, 12–17] etc.

At present, AZO thin films have been deposited on several kinds of polymer substrates including polyimide (PI) [12], polyether sulfone (PES) [13], polyethylene naphthalate (PEN) [14], polyethylene terephthalate (PET)

N. Akin (✉) · S. Sebnem Cetin · M. Cakmak · T. Memmedli · S. Ozcelik
Department of Physics, Faculty of Science, Gazi University, 06500 Teknikokullar, Ankara, Turkey
e-mail: nihanakinn@gmail.com

Table 1 Deposition parameters

Target	Al:ZnO
Substrate	ITO/PET
Base pressure of system	3.9×10^{-8} mbar
Sputtering pressure (P_S)	3.0×10^{-3} mbar
Sputtering gas	Argon
Target-substrate distance	35 mm
RF power (P_{RF})	100 W
Deposition temperature	Room temperature (RT)
Deposition rate	0.9 Å/s
Thickness of AZO thin films	25, 50, 75, 100, 125 and 150 nm

[15], polypropylene adipate (PPA) [16] and poly carbonate (PC) [17] etc. Among them, PET substrate is preferable in terms of being inexpensive, excellent in strength and superior optical properties over other polymer substrates.

In the present work, we investigated effects of the film thickness on structural, electrical and optical properties of AZO thin films deposited on ITO coated PET (ITO/PET) substrates by RF magnetron sputtering method. When we researched the results of similar studies reported in literature, we found that our results were excellent for RF-sputtered AZO thin films. In this work, the lowest electrical resistivity of the films was reached to be 2.78×10^{-5} Ω cm which is comparable to previously reported lowest values [10, 12–19]. Also, it was found that the films formed relatively strain-free interfaces which are relaxed by reducing the strain. This report may give an information about using of AZO thin films on ITO/PET substrate which is a technologically important material in flexible devices.

2 Experimental details

Aluminum doped zinc oxide (AZO) thin films were prepared by RF magnetron sputtering method under conditions listed in Table 1. A sintered oxide ceramic disk of ZnO (diameter 4 in.) mixed with 2 wt% Al_2O_3 was used as a target (purity: 99.99 %). The substrate was ultrasonically cleaned in acetone and then alcohol for 5 min respectively before it was loading into the deposition chamber.

Prior to the introduction of sputtering gas, the vacuum chamber was evacuated to 3.9×10^{-8} mbar for more than 12 h, and controlled by using an ion gauge controller. Once the desired vacuum was reached, Argon (Ar) gas was introduced into the chamber and sputtering started. Sputtering pressure (P_S) was kept at 3.0×10^{-3} mbar and the temperature of the substrate was maintained at room temperature (RT). The distance between target and substrate was about 35 mm.

Aluminum doped zinc oxide (AZO) thin films were structurally characterized by X-ray Diffractometer (XRD) and the diffraction patterns recorded on a APD 2000 PRO XRD with CuKα1 radiation (λ = 1.54178 Å) in a θ–2θ configuration. The transmittance of the film was measured by using a lambda 2S Perkin Elmer UV–visible spectrometer at RT in the range of 200–1100 nm. The resistivity, carrier concentration and Hall mobility were obtained from four-point probe and Hall Effect measurements using a Lakeshore Hall effect measurement system. The thickness of the films was measured with a stylus type profile meter (Veeco-Dektak 150).

3 Results and discussions

3.1 Structural properties

Figure 1 shows XRD pattern of bare ITO/PET and RF-sputtered AZO thin films on ITO/PET substrate at various thicknesses. It is well known that sputtered ZnO thin films are highly textured with the c-axis perpendicular to the substrate surface. In this work, all the obtained films are c-axis oriented perpendicular to the substrate surface and only exhibit the 2θ value as about 34.421 (002) plane in the XRD spectrum correspond to the ZnO pattern from the JCPDS card No. 00-036-1451. Other peaks in the pattern correspond to the ITO/PET substrates [15, 18, 19]. As exhibited in Fig. 1, with increasing film thickness, the (002) peak becomes more intense and sharper, as well as it is seen that FWHM values listed in Table 2. The 150 nm thick film has the highest and sharpest (002) peak intensity.

In order to obtain the detailed structure information, the grain size (D) was calculated along the c-axis according to the Scherrer's formula [20]:

$$D = \frac{K\lambda}{B\cos\theta} \quad (1)$$

where, K is a correction factor which was taken as 0.9, λ is wavelength of the X-ray (1.540598 Å) and B is full width at half maximum of (002) peak in the XRD pattern and θ is the Bragg angle. As shown in the inset of Fig. 1, the grain size increased from 9.20 to 44.16 nm and full width half of maximum (FWHM) decreased from 1.560 to 0.325 with increasing the film thickness (Fig. 2).

The c-axis strain (ε_{zz}) values were calculated by using biaxial strain model [21]:

$$\varepsilon_{zz}(\%) = \frac{c_{film} - c_{bulk}}{c_{bulk}} \times 100 \quad (2)$$

where, c_{film} and c_{bulk} (5.20661 as JCPDS card No. 00-036-1451) are the lattice constant c of the AZO thin films and bulk ZnO respectively, for hexagonal lattice. The biaxial

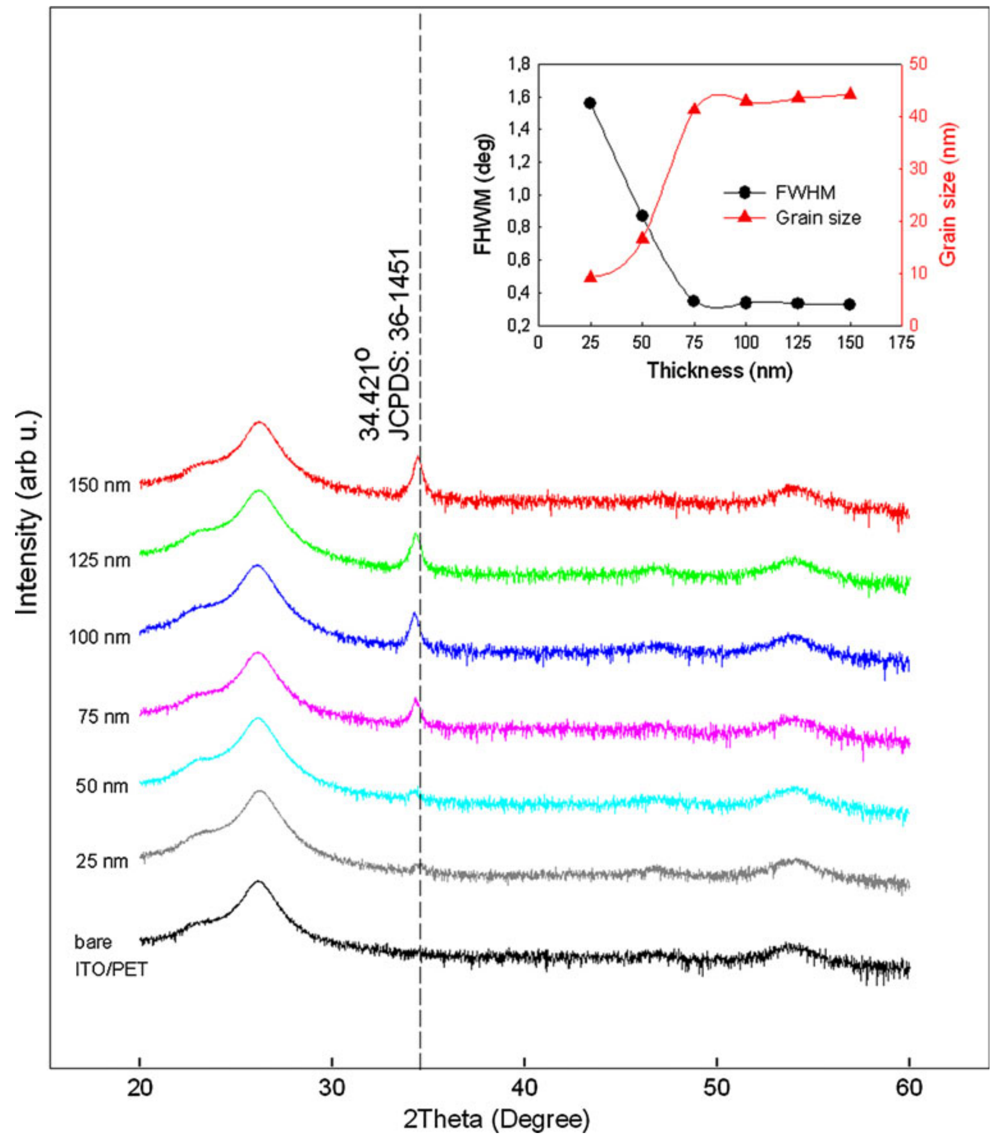

Fig. 1 XRD patterns of bare ITO/PET and RF-sputtered AZO thin films on ITO/PET substrate with various thicknesses. (*Inset* shows the change of FWHM and grain size with increasing the film thickness)

Table 2 Structural properties of AZO thin films

Thickness (nm)	2θ (deg.)	$d_{(002)}$ (Å)	FWHM (deg.)	Grain size (nm)	c_{film} (Å)	Strain (ε_{zz}) (%)	Film stress (σ_{film}) (GPa)
25	34.50	2.5976	1.560	9.2	5.1952	−0.218	0.509
50	34.28	2.6141	0.870	16.5	5.2282	0.416	−0.969
75	34.34	2.6093	0.348	41.2	5.2186	0.232	−0.540
100	34.27	2.6138	0.335	42.8	5.2276	0.405	−0.942
125	34.35	2.6083	0.330	43.5	5.2166	0.192	−0.447
150	34.44	2.6016	0.325	44.1	5.2032	−0.064	0.149

film stress (σ_{film}) values were related to the measured c-axis strain as follows [21]:

$$\sigma = \frac{2c_{13}^2 - c_{33}(c_{11} + c_{12})}{2c_{13}} \times \frac{c_{film} - c_{bulk}}{c_{bulk}} \tag{3}$$

where, c_{ij} are the elastic stiffness constants for single crystal ZnO ($c_{11} = 208.8$ GPa, $c_{33} = 213.8$ GPa, $c_{12} = 119.7$ GPa, and $c_{13} = 104.2$ GPa). Applying these values in the above equation gives the numerical relation for stress [21]:

$$\sigma_{film} = -233 \times \frac{c_{film} - c_{bulk}}{c_{bulk}} (GPa) \tag{4}$$

The calculated strain and stress values for all RF-sputtered AZO thin films were summarized in Table 2, as

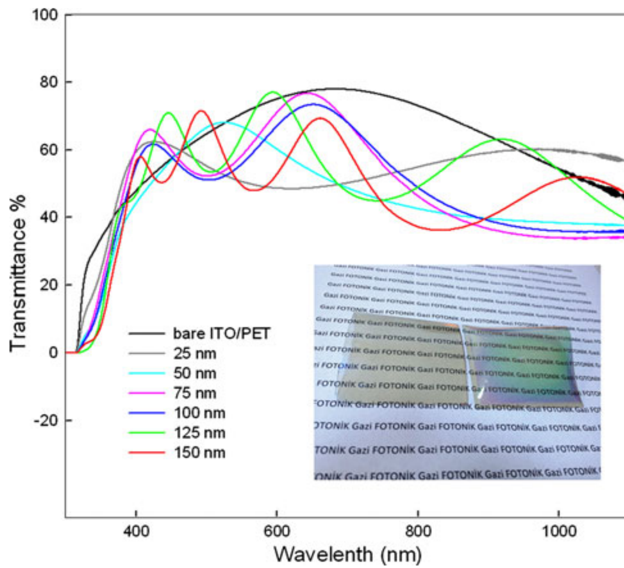

Fig. 2 The transmission spectra in the UV–VIS–IR region of the bare ITO/PET substrate and RF-sputtered AZO thin films deposited to various thicknesses. (*Inset* shows the two images: The *left image* is a bare ITO/PET substrate; the *right one* is for the ITO/PET film after the deposition)

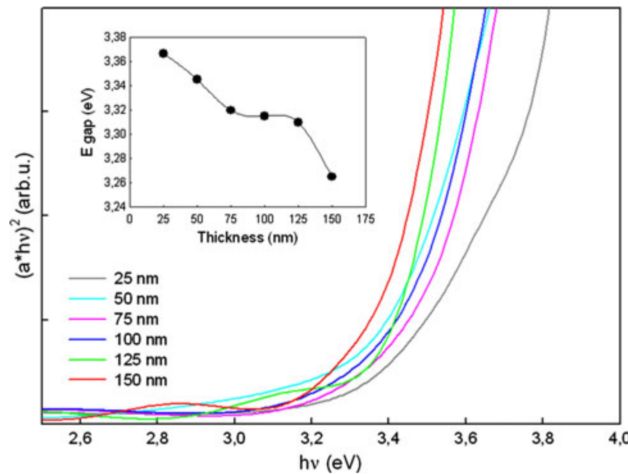

Fig. 3 Optical absorption coefficient spectra of RF-sputtered AZO thin films on ITO/PET substrate with various thicknesses

a function of the film thickness. It is seen from the calculated values that there is positive and negative stress in the AZO thin films. The positive stress denotes that the film is in tensile and the negative stress denotes compressive state of the film. As the film grows thicker above 100 nm thickness, the film is relaxed by reducing the strain. The decrease in strain indicates a decrease in the concentration of lattice imperfections because of the better crystallization.

Table 3 Hall data of AZO thin films

Thickness (nm)	Resistivity (Ω cm)	Carrier concentration (cm^{-3})	Hall Mobility (cm^2/V s)
25	2.78×10^{-5}	$3.87 \times 10^{+22}$	5.779
50	5.89×10^{-5}	$1.03 \times 10^{+22}$	10.273
75	8.05×10^{-5}	$6.96 \times 10^{+21}$	11.131
100	1.31×10^{-4}	$4.54 \times 10^{+21}$	10.463
125	1.93×10^{-4}	$3.85 \times 10^{+21}$	8.358
150	2.03×10^{-4}	$3.35 \times 10^{+21}$	9.150

3.2 Optical properties

The transmittance spectra as a function of wavelength in the range 200–1100 nm for the bare ITO/PET substrate and six samples are shown in Fig. 3. In the visible range (400–800 nm), there are some fluctuations due to the interference of light on the film/air and film/substrate interfaces. The appearance of interference fringes shows that film thickness of AZO thin films is uniform. Most fluctuations are seen in the transmittance of the 150 nm thick film. The average transmittance of the obtained AZO thin films exceeded about 75 % in the visible spectrum (400–800 nm). From the transmittance data, the band gap energies of the films were calculated by a linear fitting process. The band gap energies of AZO thin films were calculated by absorption coefficient $\alpha \sim$-ln T corresponding to the direct band gap of the wurtzite structure ZnO. It has been made a plot of $[\alpha^* (hv)]^2$ against to the photon energy hv.

As film thickness is increased, the optical band gap becomes narrower as a result of a reduction in carrier concentration, as seen from the electrical results. It is known that the optical band gap is found to be directly proportional to $N^{2/3}$ (carrier density) by linear fitting of the experimental values [22, 23]. This indicates that broadening of optical band gap at high carrier concentration. Burstein pointed out that the lifting of the Fermi level into the conduction band of the degenerate semiconductor leads to the energy band broadening (blue shift) effect. The broadening of the optical band gap is expressed as [24]:

$$\Delta E_g = \frac{h^2}{8m^*}\left(\frac{3}{\pi}\right)^{2/3} n_e^{2/3} \quad (5)$$

where, ΔE_g the shift of doped semiconductor compared to undoped semiconductor, h is the Planck's constant, m^* is the electron effective mass in conduction band, and n_e is the electron carrier concentration. The band gap is directly proportional to carrier density as seen in Eq. 5.

3.3 Electrical properties

The results of Hall measurement of RF-sputtered AZO thin films deposited on ITO/PET substrate were listed in Table 3. With increasing the film thickness, carrier

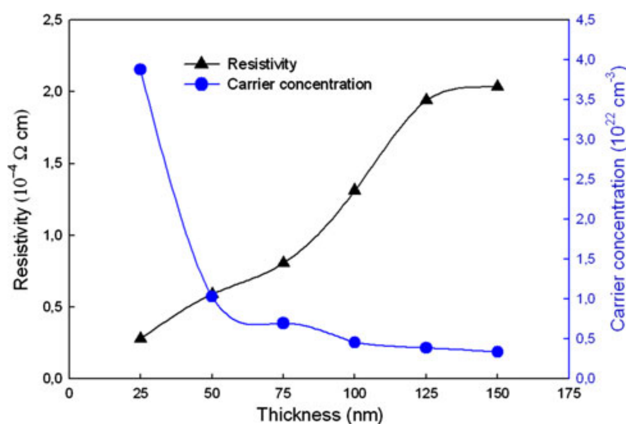

Fig. 4 Resistivity and carrier concentration of RF-sputtered AZO thin films on ITO/PET substrate with various thicknesses

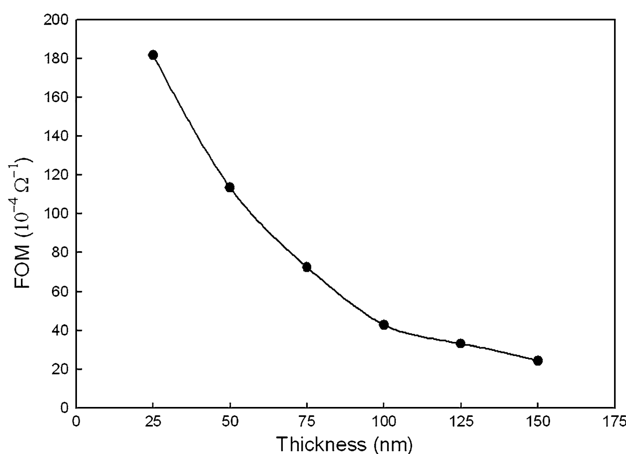

Fig. 5 Figure of merit (FOM) of RF-sputtered AZO thin films on ITO/PET substrate with various thicknesses

concentration decreases rapidly when thickness in the range from 25 to 75 nm. When the thickness is above 100 nm, carrier concentration decreases slowly and becomes almost constant. Influence of the thickness on the carrier concentration is related to variation the defect density which is interstitial and vacancies of the zinc and oxygen and also stacking defects in deposited films. The free carrier concentration is decreased with these defects acts as tarp center for the free carriers. The carrier mobility increased with film thickness in the range from 25 to 75 nm. When the thickness is above 100 nm, the mobility is decreased with the thickness of the film. The decreasing the carrier mobility may be attributed stacking defect or crack which is scatter the carriers. However, as seen in Table 3, the deposited films exhibited low resistivity. In generally, conductivity of the films is increased with increasing of the grain size in the film due to decreasing in the grain boundary scattering [25]. In contrast, resistivity of our deposited films is increased with film thickness as seen in Fig. 4. This behavior may be explained that the travel of carriers is difficult among the grains due to the increasing porosity in the film with thickness [26]. In addition, all the obtained films exhibited an n-type behavior which is in conformity with the type of conduction mechanism associated with Al doped oxide semiconductors.

For the application of flexible electronic field, transparent and conducting AZO thin films must have low resistivity and high optical transparency. In this work, this expectation confirmed by means of figure of merit (FOM) for each samples. FOM is defined by [27]:

$$FOM = T^{10}/R_S \qquad (6)$$

where, T is the average visible transmittance and R_S is the sheet resistance of the films. FOM of the RF-sputtered AZO thin films on ITO/PET substrate were exhibited in Fig. 5. Due to the lowest resistivity, the 25 nm thick AZO thin film has a maximum FOM value which fulfills the electrical and optical demands for the transparent and flexible optoelectronic device applications.

4 Conclusions

Transparent and conducting AZO thin films were successfully deposited on ITO/PET substrates by RF magnetron sputtering at RT. The film thickness dependence of the structural, optical and electrical properties of the obtained films was investigated. The obtained films were polycrystalline with the hexagonal structure and had a preferred orientation along [002] direction with the c-axis perpendicular to the substrates. The [002] peak became proportionally stronger with increasing film thickness. Calculations of the optical band gap values showed that the films had direct band gap of ranging from 3.36 to 3.26 eV. The variation in resistivity is mainly due to changes in carrier concentration. The optical band gap became narrower with increasing the film thickness due to a decrease in Burstein–Moss shift. Results proved that the RF-sputtered AZO thin films on flexible ITO/PET substrates had acceptable properties of combining the good crystallinity, high transmittance and low resistance. Therefore, this kind of TCO thin films might be probably used in flexible electronic field and this also open a new way for fabricating inexpensive flexible devices.

Acknowledgments This work was supported by the Ministry of Development of TR under Project No: 2011K120290.

References

1. E. Fortunato, L. Raniero, L. Silva, A. Goncalves, A. Pimentel, P. Barquinha, H. Aguas, L. Pereira, G. Goncalves, I. Ferreira, E. Elangovan, R. Martins, Sol. Energy Mater. Sol. Cells **92**, 1605–1610 (2008)

2. T. Minami, T. Miyata, Thin Solid Films **517**, 1474 (2008)
3. L. Gong, J. Lu, Z. Ye, Sol. Energy Mater. Sol. Cells **94**, 937–941 (2010)
4. K.I. Lee, E.K. Kim, H.D. Kim, H.I. Kang, J.T. Song, Phys. Status Solidi A **5**, 3344 (2008)
5. W.T. Lim, C.H. Lee, Thin Solid Films **353**, 12–15 (1999)
6. S.S. Shinde, K.Y. Rajpure, Appl. Surf. Sci. **257**, 9595–9599 (2011)
7. U. Ozgur, Y.I. Alivov, C. Liu, A. Teke, M.A. Reshchikov, S. Dogan, V. Avrutin, S.J. Cho, H. Morkoc, J. Appl. Phys. **98**, 041301 (2005)
8. M.B.Shahzad, Y.Qi, H.Lu, X.Wang, Thin Solid Films **534** 242–248 (2013)
9. M.E. Fragala, G. Malandrino, M.M. Giangregorio, M. Losurdo, G. Bruno, S. Lettieri, L.S. Amato, P. Maddalena, Chem. Vap. Depos. **15**, 327–333 (2009)
10. S.J. Kang, Y.H. Joung, J. Mater. Sci. Mater. Electron. **24**, 1863–1868 (2013)
11. M. Caglar, S. Ilican, Y. Caglar, F. Yakuphanoglu, J. Mater. Sci. Mater. Electron. **19**, 704–708 (2008)
12. X. Wang, X. Zeng, D. Huang, X. Zhang, Q. Li, J. Mater. Sci. Mater. Electron. **23**, 1580–1586 (2012)
13. Y.C. Lin, M.Z. Chen, C.C. Kuo, W.T. Yen, Colloids Surf. A Physicochem. Eng. Aspects **337**, 52–56 (2009)
14. J.M. Kim, P. Thiyagarajan, S.W. Rhee, Thin Solid Films **518**, 5860–5865 (2010)
15. J.Y. Kao, C.Y. Hsu, G.C. Chen, D.C. Wen, J. Mater. Sci. Mater. Electron. **23**, 1352–1360 (2012)
16. X. Hao, J. Ma, D. Zhang, T. Yang, H. Ma, Y. Yang, C. Cheng, J. Huang, App. Surf. Sci. **183**, 137–142 (2001)
17. J. Lee, D. Lee, D. Lim, K. Yang, Thin Solid Films **515**, 6094–6098 (2007)
18. A.N. Banerjee, C.K. Ghosh, K.K. Chattopadhyay, H. Minoura, A.K. Sarkar, A. Akiba, A. Kamiya, T. Endo, Thin Solid Films **496**, 112–116 (2006)
19. S. Fernandez, A.M. Steele, J.J. Gandiz, F.B. Naranjo, Thin Solid Films **517**, 3152 (2009)
20. H.P. Klug, L.E. Alexander, *X-ray Diffraction Procedures* (Wiley, New York, 1974)
21. R. Cebulla, R. Wendt, K. Ellmer, J. Appl. Phys. **83**, 1087 (1998)
22. H.T. Cao, Z.L. Pei, J. Gong, C. Sun, R.F. Huang, L.S. Wen, Surf. Coat. Technol. **184**, 84 (2004)
23. Q.B. Ma, Z.Z. Ye, H.P. He, S.H. Hu, J.R. Wang, L.P. Zhu, Y.Z. Zhang, B.H. Zhao, J. Cryst. Growth **304**, 64–68 (2007)
24. B.Y. Oh, M.C. Jeong, D.S. Kim, W. Lee, J. Min, J. Cryst. Growth **281**, 475–480 (2005)
25. Z. Huafu, L. Chengxin, L. Hanfa, Y. Changkun, J. Semicond. **30**, 0430041–0430044 (2009)
26. A. Zhong, J. Tan, H. Huang, S. Chen, M. Wang, S. Xu, App. Surf. Sci. **257**, 4051–4055 (2011)
27. G. Haacke, J. Appl. Phys. **47**, 4086–4089 (1976)